CHEMISTRY
A European Journal

A Journal of
ChemPubSoc Europe

Accepted Article

Title: Bis[1]benzothieno[1,4]thiazines – Planarity, Enhanced Redox Activity and Luminescence by Thieno-Expansion of Phenothiazine

Authors: Arno P. W. Schneeweis, Simone T. Hauer, Guido J. Reiss, and Thomas J. J. Müller

To be cited as: *Chem. Eur. J.* 10.1002/chem.201805085

Link to VoR: http://dx.doi.org/10.1002/chem.201805085

Supported by
ACES

WILEY-VCH

10.1002/chem.201805085

WILEY-VCH

Bis[1]benzothieno[1,4]thiazines – Planarity, Enhanced Redox Activity and Luminescence by Thieno-Expansion of Phenothiazine

Arno P. W. Schneeweis,[a] Simone T. Hauer,[a] Guido J. Reiss,[b] and Thomas J. J. Müller*,[a]

Abstract: Twofold *Buchwald-Hartwig* aminations selectively furnish all three regioisomers of bis[1]benzothieno[1,4]thiazines and X-ray structure analyses and DFT calculations were corroborated for correlation of their electronic properties. All regioisomers outscore the parent compound phenothiazine with respect to a low lying oxidation potential and reversible redox activity. The *anti-anti* bis[1]benzothieno[3,2-*b*:2',3'-*e*][1,4]thiazines possess the lowest oxidation potentials in this series and display pronounced green luminescence in solution ($\Phi_F \approx 20\%$) and in the solid state. *Syn-anti* regioisomers are only weakly luminescent in solution, but show aggregation induced emission enhancement and solid state luminescence. Most interestingly, found by X-ray structure analyses *anti-anti* derivatives reveal an amazingly coplanar structure of the pentacyclic anellated 1,4-thiazine system, emphasizing a structural similarity to heteroacenes. The calculated theoretical nucleus-independent chemical shifts additionally suggest that these 8π-electron core systems can be considered as the first electronically unbiased anellated 1,4-thiazines with antiaromatic character.

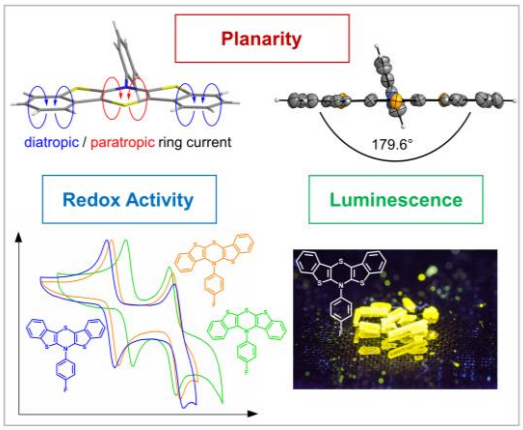

Introduction

Electron-rich heterocycles adopt a prominent role in organic electronics, and already find numerous applications in photonics and photovoltaics.[1] As organic donors with inherently reversible oxidation potentials di- and tri(hetero)arylamines match excellently with required electronic profiles.[2] Interestingly, anellated 1,4-thiazines, like phenothiazine, according to higher semiquinone formation constants, form more stable reversible redox systems than many other di- and triarylamines.[3] Phenothiazine, a classic tricyclic heteroarene with a pronounced pharmacological profile,[4] can be readily modulated as a donor moiety in functional π-systems.[5] The major challenge of designing novel anellated 1,4-thiazine donors remains in providing lower oxidation potentials than phenothiazine. Thieno anellation of the 1,4-thiazine core furnishes dithieno[2,3-*b*:3',2'-*e*][1,4]thiazines.[6] Formal replacement of the benzo moiety by the higher polarizable thiophene core consequently leads to a significant cathodic shift, i.e. a decrease, of the oxidation potential. However, on expense of the thieno anellation luminescence characteristics typical for many phenothiazines were significantly minimized. Yet, luminescence could be restored after specific (hetero)aryl substitution at the α-positions.[6] Therefore, we conceptualized restoring of luminescence by anellation of an extended π-system to 1,4-thiazine. Based on the phenothiazine core structure, we reasoned an expansion of the π-system by formal insertion of thiophene rings furnishing bis[1]benzothieno[1,4]thiazines (BBTT), structural and electronic combinations of both phenothiazine and dithieno[1,4]thiazine (Figure 1). These pentacyclic π-systems share topological similarities with the highly topical class of heteroacenes,[7] which became increasingly important as semiconducting materials in organic field-effect transistors.[8] Herein, we present the first syntheses of three regioisomeric bis[1]benzothieno[1,4]thiazines and investigations on their ground and excited state electronic properties and electronic structure.

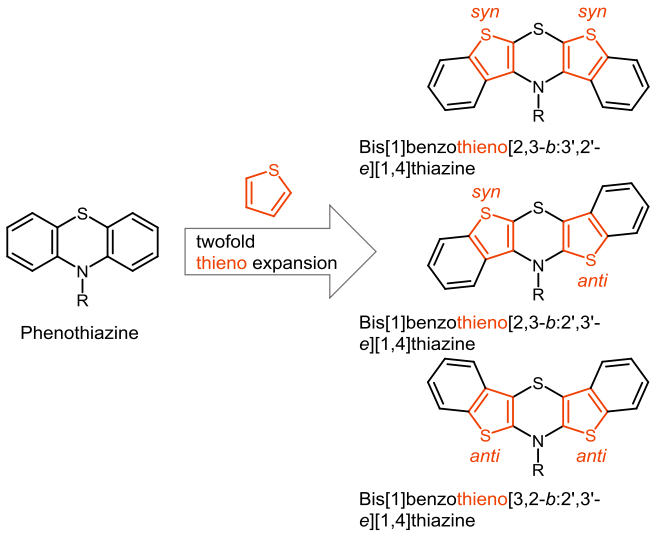

Figure 1. Bis[1]benzothieno[1,4]thiazines – doubly thieno-expanded phenothiazines with *N*-substitution.

[a] M. Sc. A. P. W. Schneeweis, S. T. Hauer, Prof. Dr. T. J. J. Müller
Institut für Organische Chemie und Makromolekulare Chemie
Heinrich-Heine-Universität Düsseldorf
Universitätsstraße 1, D-40225 Düsseldorf, Germany.
E-Mail: ThomasJJ.Mueller@hhu.de

[b] Dr. G. J. Reiss
Institut für Anorganische Chemie und Strukturchemie
Heinrich-Heine-Universität Düsseldorf
Universitätsstraße 1, D-40225 Düsseldorf, Germany.

Results and Discussion

Synthesis

The three regioisomers bis[1]benzothieno[2,3-*b*:3',2'-*e*][1,4]thiazine, bis[1]benzothieno[2,3-*b*:2',3'-*e*][1,4]thiazine, and bis[1]benzothieno[3,2-*b*:2',3'-*e*][1,4]thiazine differ by the mode of anellation of the benzo[*b*]thiophene unit at the central 1,4-thiazine core (Figure 1). According to the orientation of the thiophene rings with respect to the 1,4-thiazine sulfur these regioisomers are abbreviated as *syn-syn*, *syn-anti*, and *anti-anti* BBTT for simplification. Motivated by quantum chemical calculations on 4*H*-dithieno[2,3-*b*:3',2'-*e*][1,4]thiazine and our syntheses of its derivatives the synthetic approach to BBTT derivatives was pursued accordingly.[6] All regioisomers of BBTT can be convergently synthesized by an intermolecular-intramolecular[9] *Buchwald-Hartwig* amination[10] using the respective dibrominated starting materials[11] and various *para*-substituted anilines. This concise synthetic strategy allows a facile variation of the *N*-substituent (Scheme 1), thus enabling fine-tuning of the electronic properties of the π-system. According to optimization studies the right choice of the employed ligand for Pd catalyst is crucial for obtaining satisfying yields of the desired BBTT. As a consequence of inherent steric hindrance *syn-syn* BBTTs are generally formed in lower yields compared to the other two regioisomers (see also Figure 2).

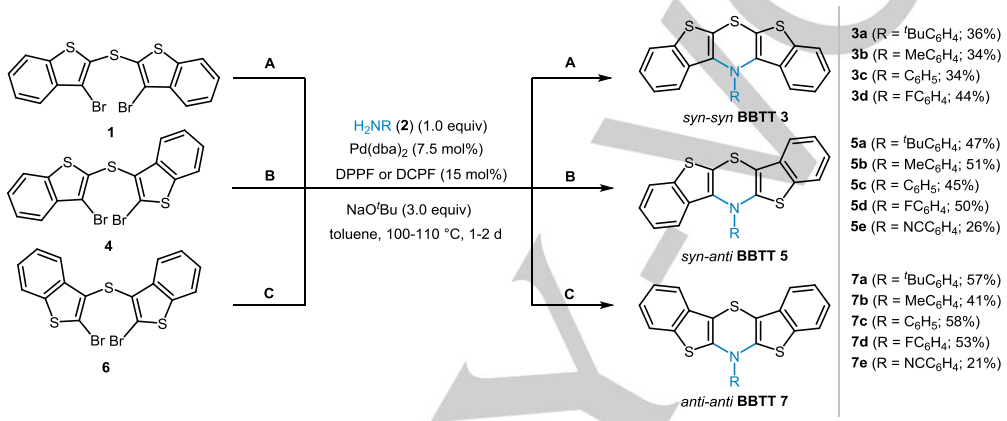

Scheme 1. Selective synthesis of the three BBTT regioisomers by twofold *Buchwald-Hartwig*-amination (yields are given after isolation by flash chromatography and recrystallization; ligands used for the syntheses: route **A** and **B** 1,1'-bis(dicyclohexylphosphano)ferrocene (DCPF) and route **C** 1,1'-bis(diphenylphosphano)ferrocene (DPPF).

Structure

The structures of the three regioisomers **3**, **5**, and **7** were corroborated by X-ray structure analyses of several differently substituted examples (Figure 2).[12] Benzothieno anellated 1,4-thiazines are characterized by their significant folding along the S-N axis with folding angles θ of these butterfly-like conformations, as well as torsion (α) and orientation (β) angles of the *N*-aryl substituents (Table 1).[13]

Table 1. Selected folding, torsion and orientation angles determined by X-ray structure analyses.

Compound	folding angle θ [°]	torsion angle α [°]	S-N-C_{phenyl} angle β [°]
3a[a]	136.9	87.2	111.5
	131.8	81.3	115.0
3d	125.8	88.9	120.6
5d	136.5	64.8	128.5
5d	166.0	34.3	136.5
7a	177.6	1.5	177.9
7c	179.6	35.8	167.0
7d[a]	159.2	3.3	168.5
	155.6	20.0	167.1
7e	175.0	59.8	167.9
N-phenylphenothiazine[a][14]	162.6	-	-
	150.7		

[a] Two molecules are found in the asymmetric unit of the single crystal.

The conformation of anellated 1,4-thiazines in the solid state can be classified as *intra* (quasi-equatorial) or *extra* (quasi-axial) (see Figure 2).[6b,14-15] Due to steric hindrance between the *N*-substituent and the benzo[*b*]thiophene wings the *syn-syn* BBTTs **3a** and **3d** adopt *extra* conformations in the solid state. The same reasoning can be applied for the *syn-anti* BBTT **5d** with a more relaxed *extra* conformation due to less steric hindrance. Finally, the crystal structure of the *anti-anti* BBTT **7d** adopts an *intra* conformation, as a consequence of the absence of steric biases. The *intra* conformation induces a larger folding angle θ and, therefore, increasing the interaction of 1,4-thiazine sulfur and nitrogen with the fused π-systems. This conformationally induced interaction considerably influences the electronic properties (vide infra, Figure 5).

Surprisingly, X-ray crystal structures of *anti-anti* BBTTs (**7a**, **7c**, **7e**) reveal almost completely coplanar conformations of the pentacyclic core systems. For the crystals of **7c** a remarkably high folding angle θ of 179.6° is found. Although thermal ellipsoids of sulfur and nitrogen atoms indicate a certain deviation of these atoms from the benzo[*b*]thiophene plane, intermolecular interactions of the molecules in the crystals were excluded by inspection of the shortest distances between the □-system in the X-ray structures of **7a** (3.59 Å), **7c** (3.60 Å) and **7e** (3.5 Å), i.e. larger distances than the *van der Waals* distance between two sp^2-hybridized carbon atoms (3.4 Å)[16] (for an illustration see supporting information). For the *p*-cyano-substituted derivative **7e** the molecular distance is the shortest indicating more intermolecular interactions in the crystal.

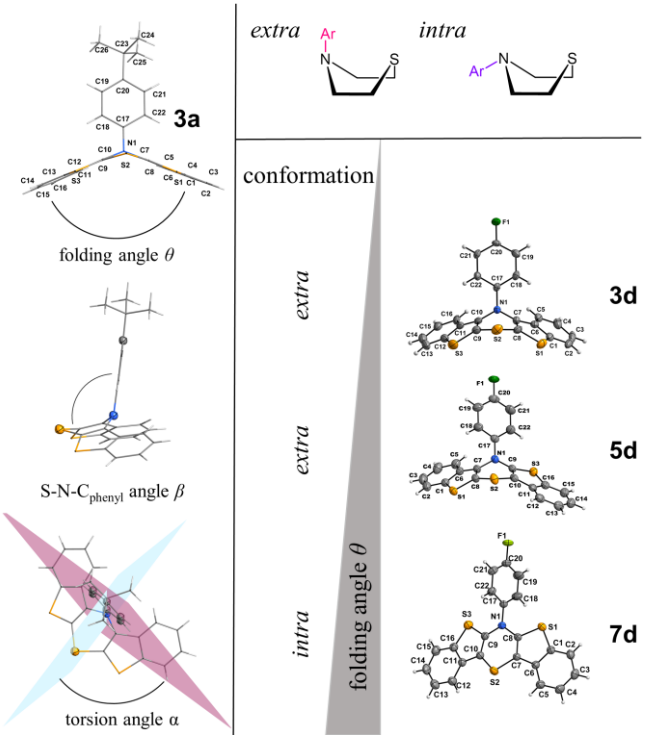

Figure 2. Crystal structures of compounds **3a**, **3d**, **5d**, and **7d** and illustration of the angles shown in Table 1.

Planar 1,4-thiazine derivatives can be considered to be inherently antiaromatic as a consequence of the 8π-electron system and they are not known in the literature. Only by electronic biases, such as strongly electron withdrawing substituents, 1,4-thiazines can adopt planar conformations, e.g. for *p*-nitrophenyl substituted diquino[1,4]thiazines.[17] However, the discussed anellated 1,4-thiazines, such as *anti-anti* BBTTs **7a** and **7c**, are electron-rich systems bearing electron neutral substituents at the nitrogen center. The observed exceptional planarity of compounds **7a**, **7c**, and **7e** raises the question about their degree of antiaromaticity. Therefore, the antiaromaticity of the 1,4-thiazine core was assessed by well-established theoretical nucleus-independent chemical shifts (NICS) calculations.[18]

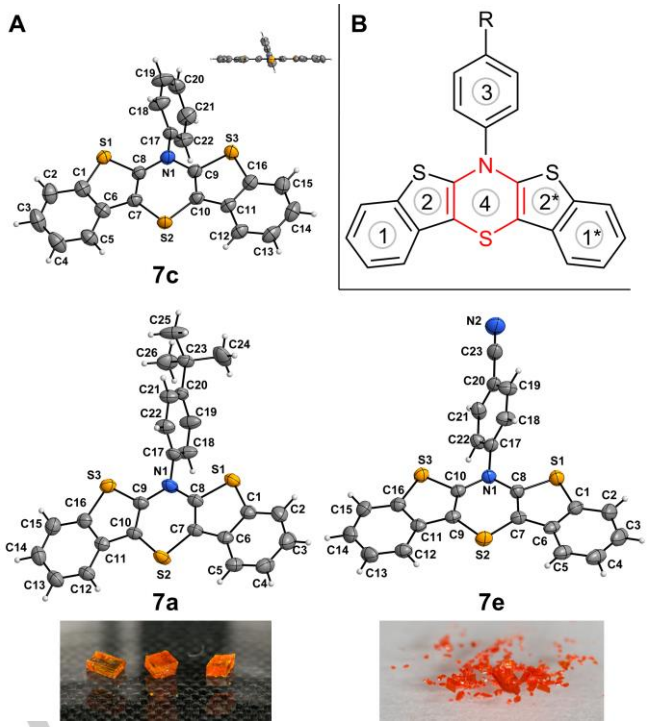

Figure 3. (A) Crystals and crystal structures of the planar *anti-anti* BBTTs **7a**, **7c** and **7e**. (B) Placement and numbering of ghost atoms used for NICS calculations (see Table 2).

For structures **7a**, **7d**, and **7e** the NICS(0) and NICS(1) (1 Å above (+1) and under (-1) the plane) method was tested using the GIAO protocol in the Gaussian 09 package[19] with RB3LYP[20]/6-311+G**.[21] The starting geometries were extracted from the respective crystal structures and minimum structures were examined by frequency analyses. NICS calculations were performed for all six rings (Table 2). The positive NICS(0) and NICS(1) values for the 1,4-thiazine rings strongly suggest a significant paratropic ring current. To exclude that the calculated positive NICS values of the 1,4-thiazine are primarily caused by the neighboring aromatic thiophene ring currents a system based on two benzo[b]thiophenes with the same coordinates as the benzo[b]thiophene wings of the BBTT and the same placement of ghost atoms (benzo[*b*]thiophene dimer test system) was used for NICS calculations (see supporting information). According to the NICS(1) values the calculated paratropic ring current of in the center of BBTTs is mainly caused by the ring current of the 1,4-thiazine. Therefore, the central cores of all three molecules **7a**, **7d**, and **7e** are plausibly assumed to be antiaromatic.

Table 2. Calculated NICS values of **7a**, **7c**, and **7e** (RB3LYP/6-311+G**).

Ring No.	**7a** NICS(0/+1/-1)	**7c** NICS(0/+1/-1)	**7e** NICS(0/+1/-1)	benzo[*b*]thiophene dimer test system NICS(0/1)	Ring current	Aromaticity
1	-8.42/-10.37/-10.32	-8.42/-10.35/-10.45	-8.37/-10.38/-10.26	-8.48/-10.81	diatropic	aromatic
1*	-8.47/-10.47/-10.27	-8.57/-10.32/-10.26	-8.29/-10.32/-10.37	-8.39/-10.85	diatropic	aromatic
2	-9.50/-6.66/-6.76	-9.21/-6.67/-7.05	-8.44/-6.88/-6.37	-11.34/-8.13	diatropic	aromatic
2*	-9.46/-6.93/-6.91	-9.48/-6.49/-6.56	-8.39/-6.88/-6.11	-11.20/-9.15	diatropic	aromatic
3	-8.08	-7.61	-7.50	-	diatropic	aromatic
4	+8.32/+7.17/+7.18	+7.56/+6.50/+6.85/	+6.35/+6.13/+5.57	+4.53/+2.02	paratropic	antiaromatic

10.1002/chem.201805085

Electronic Properties and Electronic Structure

The electronic properties of the three BBTT regioisomers **3**, **5**, and **7** were examined in solution by cyclic voltammetry (Table 3), UV/Vis and fluorescence spectroscopy. All BBTTs show two fully chemical reversible oxidation processes (Figure 4A). Moreover, the first and second oxidations of *syn-anti* and *anti-anti* BBTTs are *Nernstian* reversible. In case of the *syn-syn* BBTT the first oxidation is quasi-reversible whereas the second oxidation is *Nernstian* reversible (for a detailed illustration see supporting information). In comparison to *N*-phenylphenothiazine, all *N*-phenyl BBTT regioisomers show lower potentials for the first and second oxidations.[6a] However, in comparison to the respective dithieno[2,3-*b*:3',2'-*e*][1,4]thiazines the first oxidation potentials are shifted anodically. These findings are in agreement with the potential differences between dithieno[3,2-*b*:2',3'-*d*]pyrroles and bis[1]benzothieno[3,2-*b*:2',3'-*d*]pyrroles.[22] In the series of the three regioisomers *anti-anti* BBTTs are easiest to oxidize (for HOMO energy levels see supporting information). Interestingly, the gap of the first potential is largest between the *syn-syn* and the *syn-anti* BBTT, also as a consequence of largest structural differences between these two regioisomers. The comparison of the second oxidation potentials reveals a reversed order for the regioisomers. The radical cations of the *syn-syn* BBTTs are generally easier to oxidize than the radical cations of the *syn-anti* and *anti-anti* regioisomers.

Table 3. First and second oxidation potentials of the three regioisomers **3**, **5**, and **7** (referenced to internal standard decamethylferrocene[23] E_0 = –552 mV (vs. ferrocene[24] $E_0(Fc/Fc^+)$ = 0 V)), and semiquinone formation constant K_{SEM} ($K_{SEM} = 10^{\frac{(E_0^{0/+1} - E_0^{+1/+2})}{0.059\ V}}$).

Compound / R	$E_0^{0/+1}$ [V]	$E_0^{+1/+2}$ [V]	K_{SEM}
3a / ^{t}Bu	0.17	0.67	$3.0 \cdot 10^8$
3b / Me	0.15	0.67	$6.5 \cdot 10^8$
3c / H	0.19	0.67	$1.4 \cdot 10^8$
3d / F	0.21	0.68	$9.2 \cdot 10^7$
5a / ^{t}Bu	0.00	0.71	$1.1 \cdot 10^{12}$
5b / Me	0.00	0.71	$1.1 \cdot 10^{12}$
5c / H	0.03	0.72	$5.0 \cdot 10^{11}$
5d / F	0.05	0.72	$2.3 \cdot 10^{11}$
5e / CN	0.20	0.76	$3.1 \cdot 10^9$
7a / ^{t}Bu	-0.04	0.73	$1.1 \cdot 10^{13}$
7b / Me	-0.04	0.73	$1.1 \cdot 10^{13}$
7c / H	-0.02	0.74	$7.6 \cdot 10^{12}$
7d / F	0.01	0.75	$3.5 \cdot 10^{12}$
7e / CN	0.09	0.78	$5.0 \cdot 10^{11}$
N-phenylphenothiazine[6a]	0.27	1.07	$3.6 \cdot 10^{13}$
N-phenyl-dithieno[1,4]thiazine[6a]	-0.06	0.81	$5.6 \cdot 10^{14}$

From the differences of first and second oxidation potentials the semiquinone formation constants K_{SEM} can be calculated.[25] A higher semiquinone formation constant indicates a higher stability of the radical cation against disproportionation into the reduced form and the dication. Here, the K_{SEM} values indicate that the *anti-anti* regioisomers **7** form most stable radical cations. The comparison of the cyclic voltammograms of *syn-syn* and *anti-anti* BBTTs **3b** and **7b** evaluated by semi-differential deconvolution[26] (Figure 4B) allows for a qualitative discussion of electron transfer processes at the anode. The higher peak separation for $E_0^{0/+1}$ of *syn-syn* BBTT **3b** in comparison to $E_0^{+1/+2}$ indicates that the first oxidation process to give the radical cation is inhibited. In analogy to phenothiazine this inhibition corresponds to the barrier of structural changes from the butterfly conformation of the reduced species to the planarized radical cation.[27] Taking into account steric hindrance in neutral *syn-syn* BBTT the structural changes required for planarization should additionally hamper the first oxidation. In the subsequent second oxidation process to furnish the dication, no major structural changes are expected. The *anti-anti* regioisomer **7b** experiences a drastically reduced steric hindrance by the *N*-phenyl substituent, favoring the molecule's *intra* conformation. Consequently, less structural reorganization upon oxidation is required for a planarization. Therefore, the electron transfer to the electrode surface is almost non-inhibited, a favorable feature for all relevant electron transfer processes in electronic materials.

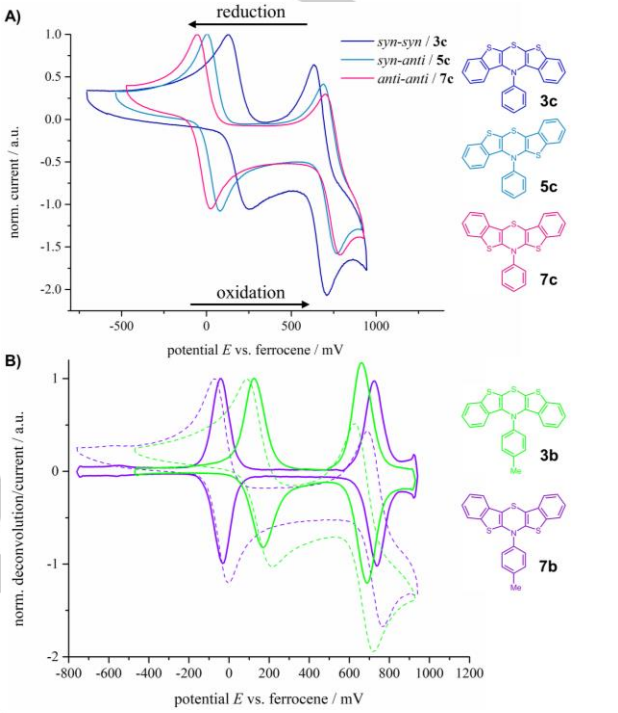

Figure 4. (A) Cyclic voltammograms of compounds **3c**, **5c** and **7c**. (B) Deconvolution diagram and cyclic voltammograms of **3b** and **7b** (CVs recorded in CH_2Cl_2, rt, electrolyte 0.1 M [*n*-Bu_4N][PF_6]; ν = 100 mV/s; Pt working and counter electrode, Ag/AgCl reference electrode, referenced to decamethylferrocene[23] E_0 = -552 mV (vs. ferrocene[24] $E_0(Fc/Fc^+)$ = 0 V)).

Different anellation and substitution patterns of the BBTT derivatives strongly affect the electronic ground state, and likewise also the electronic excitations, and, thus, a significant influence on the excited state properties can be expected. This effect is nicely reflected by the UV/Vis spectra of the three regioisomers (Figure 5). As a consequence of the more planar structure the interactions between the heteroatoms of the 1,4-thiazine and π-systems is increased and, thus, the longest wavelength absorption bands of the *anti-anti* derivatives **7** are redshifted. Additionally, the conjugation pathway between the nitrogen electron pair and the benzo[*b*]thiophene wing is best for the *anti*-orientation.

10.1002/chem.201805085

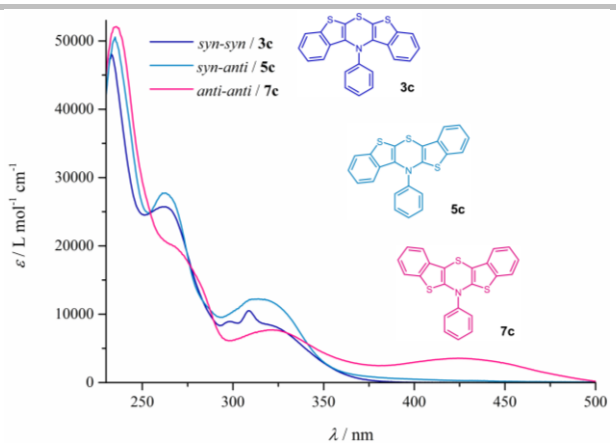

Figure 5. UV/Vis spectra of compounds **3c**, **5c** and **7c** (recorded in CH_2Cl_2).

In contrast to *N*-aryl substituted dithieno[1,4]thiazine derivatives BBTTs indeed reveal a distinct emission behavior.[6a] All *syn-syn* BBTTs **3** do not show measurable emission in solution upon UV excitation. However, the *syn-anti* BBTTs **5** are weakly orange fluorescent with remarkably large *Stokes* shifts up to 8000 cm^{-1} (Figure 6A), a typical feature of phenothiazines.[28] Here, the electron deficient cyano derivative **5e**, which is essentially non-fluorescent in solution, is an exception.

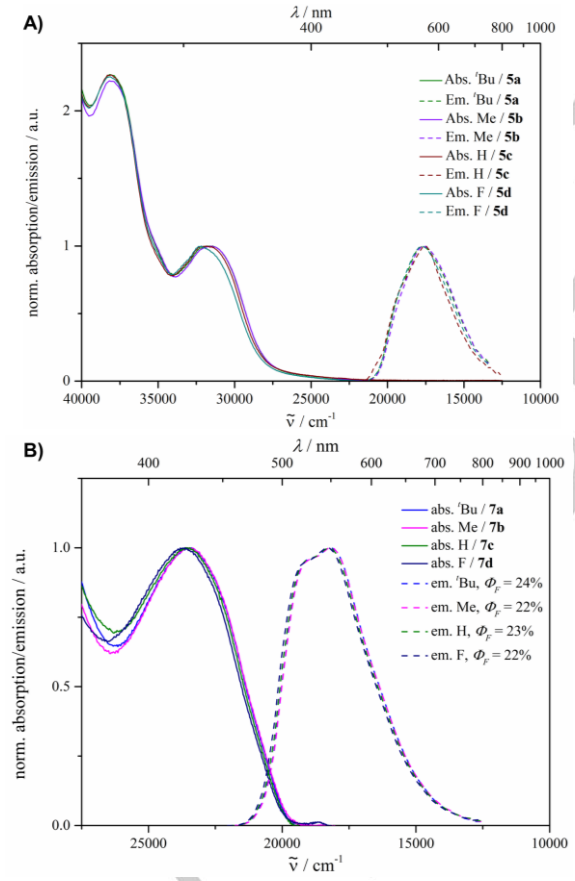

Figure 6. (A) Normalized absorption and emission spectra of *syn-anti* derivatives **5**. (B) Normalized absorption and emission spectra of *anti-anti* derivatives and determined quantum yields Φ_F (recorded in CH_2Cl_2, absolute Φ_F: **7a**, **7c**, **7d**; relative Φ_F (**7b**) determined with coumarin 153 as a standard in MeOH (Φ_F = 0.45)[29].

Most impressively, the emission behavior of *anti-anti* BBTT derivatives **7** is clearly superior to the other two regioisomers (Figure 6B), with exception the *p*-cyano derivative **7e**, which is essentially non-emissive in solution and in the solid state. The other derivatives **7** generally display green emission upon excitation with UV light and notably higher quantum yields in the range of 20% are measured. Additionally, the *Stokes* shifts are drastically lower and range from 5300 to 5400 cm^{-1}. Anellated 1,4-thiazines, such as phenothiazine without any additional functionalization of the anellated π-system, normally reach only lackluster fluorescence quantum yields, while the dithieno[1,4]thiazine is essentially non-luminescent. The *anti-anti* BBTTs **7** easily surpass similar substituted phenothiazines in terms of fluorescence quantum yields.[30]

In the emission data ($\lambda_{max,em}$ and fluorescence quantum yields Φ_F) no major influence of the corresponding *para*-substituents is found. TD-DFT calculations were performed for exploring the electronic nature of the vibrationally relaxed first excited state of *anti-anti* BBTT **7c** (Figure 7). The *Franck-Condon* excitation at 423 nm ($\lambda_{max,exp}$ = 424 nm) can be considered as a HOMO → LUMO (96%, *f* = 0.1507) transition, which is associated with a characteristic transfer of electron coefficient density from the 1,4-thiazine ring (HOMO) to the benzo[*b*]thiophene wings (LUMO). This is generally considered as a charge transfer transition. The vibrationally relaxed S_1 geometry is essentially planar in the pentacyclic bis[1]benzothieno[1,4]thiazine moiety. Excitation from the vibrationally excited ground state S_0* to the relaxed first excited state S_1 translates into the process of fluorescence. The involved HOMO → LUMO transition (99%, *f* = 0.1754, λ_{calc} = 585 nm, $\lambda_{max,exp}$ = 549 nm) reveals almost no distribution of electron coefficient density on the *N*-phenyl substituent. Therefore, the electronic effect of *p*-phenyl substitution only has a minimal impact on the fluorescence, which nicely rationalizes the experimental observations. However, functionalization at the bis[1]benzothieno[1,4]thiazine core system still needs exploration.

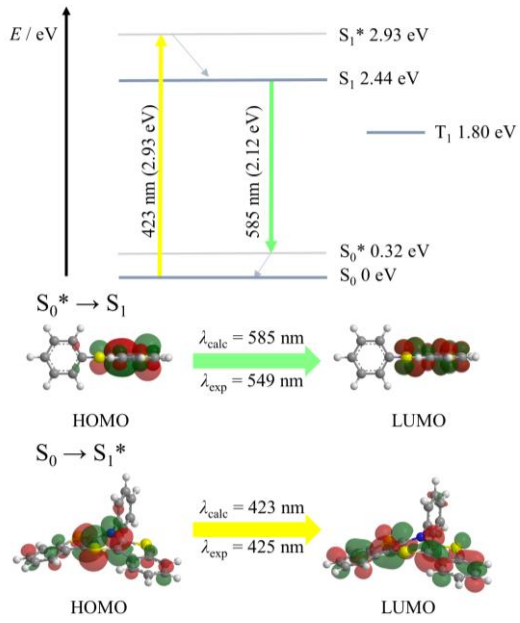

Figure 7. *Jablonski* diagram of compound **7c** ($E(S_0)$ = 0 eV; B3LYP/6-311++G** IEFPCM CH_2Cl_2, isosurface value at 0.03 a.u.).

10.1002/chem.201805085

Just like in solution, the crystals of the *para*-substituted *syn-syn* derivatives **3** are essentially non-emissive. The maxima of emissive crystals of *syn-anti* derivatives **5** are generally blue-shifted and the fluorescence quantum yield in the crystal state is apparently higher than in solution.

Moreover, crystallization of the *p*-fluoro-substituted BBTT **5d** led to the formation of two polymorphs,[31] which were analyzed by X-ray diffraction and emission spectroscopy. The bright yellow single crystals of **5d** exhibit green fluorescence similar to the yellow crystals of *p*-methyl-substituted BBTT **5b** (Φ_F = 7%) with increased quantum yields of 6%, while the colorless single crystals of **5d** show red-shifted orange fluorescence with lower quantum yields of only 2% (Figure 8). The molecules in the asymmetric unit of the two crystal structures display major conformational differences. The BBTTs in colorless crystals are significantly more folded (θ = 136.5°) than molecules in bright yellow crystals (θ = 166.0°). Additionally, there are differences in the orientation of the *N*-phenyl substituent represented by the α angle (Table 1) allowing different interactions between the nitrogen lone pair and the π-system of the *N*-substituent. The influence of the different ground state geometries on the excitation properties was explored by TD-DFT calculations (B3LYP/6-311++G**) using the corresponding crystal geometries of **5d**. For the colorless crystals a longest wavelength absorption band at 364 nm was calculated (HOMO → LUMO (95%, *f* = 0.0031). According to the optical appearance of the bright yellow crystals a bathochromically shifted longest wavelength absorption band at 410 nm (HOMO → LUMO (98%), *f* = 0.0019) was determined (see Supp Inf for plots of the associated frontier orbitals).

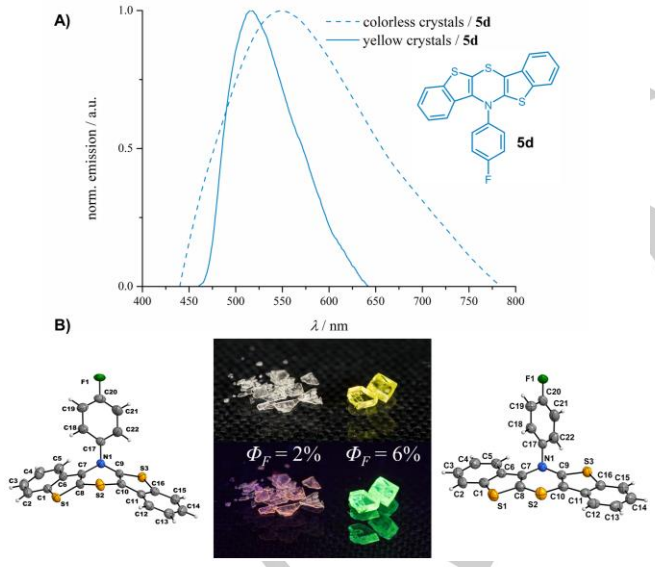

Figure 8. (A) Normalized emission spectra of the two crystal types of **5d**. (B) The two crystal types of **5d** (above: daylight; below: UV-light λ_{exc}= 365 nm; absolute Φ_F of the crystals) and their associated crystal structures.

The apparent and measurable difference in fluorescence of the presented polymorphs is obviously based on geometrical changes between ground state and the assumed planar geometry of the common vibrationally relaxed excited state S_1. The higher geometrical deviation between ground and planar excited state translates into a larger *Stokes* shift and pronounces the red shift from green to orange fluorescence. In addition, the larger geometry change also causes a lower solid state fluorescence quantum yield of 2%.

The emissive properties of the crystals of the *anti-anti* BBTTs depend on the crystal type. The yellow crystals of the *p*-fluoro-substituted BBTT **7d** display yellow fluorescence with only a minor loss of quantum yield (Φ_F = 16%) in comparison to emission in solution (Φ_F = 22%). The corresponding crystal structure is similar to the calculated structure in solution. However, the orange crystals of the antiaromatic derivatives **7a** (Figure 9) and **7c** show bathochromically shifted emission with diminished quantum yields (Φ_F (**7a**) = 10%; Φ_F (**7c**) = 5%). The *Stokes* shift in the crystals (2700 cm^{-1}) is significantly lower compared to the *Stokes* shift in solution (5300 cm^{-1}) caused by the structural similarity between the planar ground state geometry in the solid state (see Figure 3) and the planar vibrationally relaxed excited state geometry (see Figure 7). Furthermore, the influence of the planar structure on the optical properties of the crystals was additionally corroborated by TD-DFT calculations (RB3LYP/6-311++G**). The orange color of the crystals of compound **7a** (Figure 9) is nicely reproduced (λ_{calc} = 460 nm, HOMO → LUMO, 98%, *f* = 0.1094) when employing the X-ray data as a starting geometry.

Fluorescence intensities of the crystals of the *syn-anti* derivatives **5** are higher than in solutions of the same compounds. Consequently, aggregates of the chromophores should also express intensive fluorescence.[32] Indeed, the fluorescence of *syn-anti* BBTT **5d** is significantly enhanced by the formation of aggregates, i.e. aggregation induced enhanced emission (AIEE).[33] An AIEE titration experiment visualizes this effect (Figure 10A). For a given concentration of *syn-anti* BBTT **5d** various ratios of binary THF/water mixtures indicate the formation of fluorescent aggregates and thus unambiguously identifying AIEE behavior (Figure 10B). Further assessments of this unusual luminescence effect will be studied in more detail in ongoing investigations.

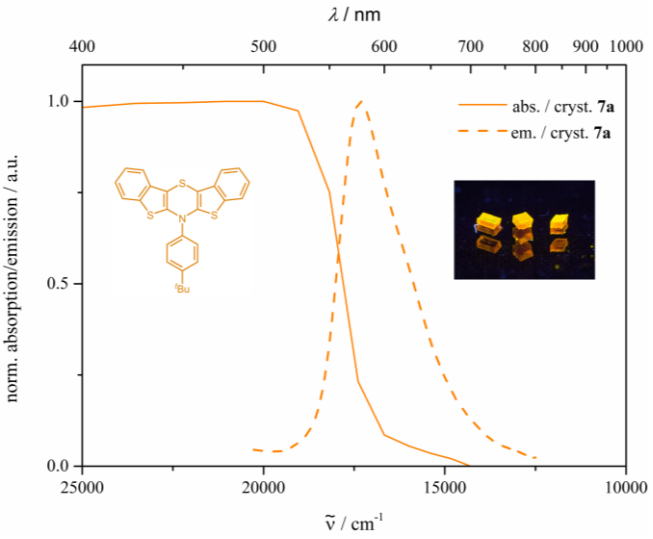

Figure 9. Normalized excitation (solid line) and emission (dashed line) spectra of the orange crystals of **7a** (Φ_F = 10%).

10.1002/chem.201805085

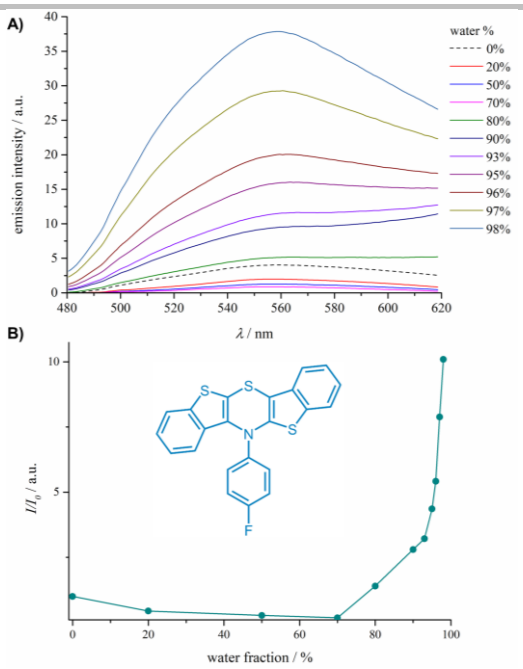

Figure 10. AIEE experiments: (A) Emission spectra of **5d** in THF with different water fractions (c(**5d**) = 6 · 10^{-5} mol/L). (B) Plots of I/I_0 of **5d** vs. water fractions in THF/water mixtures (I_0 = emission intensity in pure organic solvent, I = emission intensity in water mixture).

Conclusion

In summary, all three regioisomers of bis[1]benzothieno[1,4]thiazine (BBTT) were selectively synthesized by twofold *Buchwald-Hartwig* amination and their structures were extensively characterized by X-ray structure analyses. Although, all three regioisomers share many similarities with respect to their electronic properties they also display distinct peculiarities as a consequence of their mode of anellation. While *syn-syn* BBTTs are essentially non-luminescent, the emission behavior is restored for *syn-anti* and *anti-anti* BBTTs in solution and often also in the solid state. Besides distinct solid state emission also polymorphous emission was observed for the *p*-fluoro-substituted *syn-anti* BBTT derivative. X-ray structure analyses and DFT calculations additionally support the influence of structural features on the excitation properties of the molecule in the solid state. It is noteworthy to mention that some of the solid state emissive derivatives display AIEE, a particularly favorable feature for application in fluorescence sensor systems.[34]
Finally, three planar antiaromatic *anti-anti* BBTTs were identified by X-ray structure analyses and the antiaromatic character of these systems was assessed by NICS(0) and NICS(1) calculations. Further efforts to enhance the fundamentally interesting inherent antiaromaticity, also with respect to small singlet-triplet separations, as well as enhancing the optical and materials properties of novel multifunctional π-systems are currently underway.

Supporting information for this article is available on the WWW under http://dx.doi.org/10.1002/chem.2014xxxxx. Experimental details and full characterization of BBTTs **3**, **5**, and **7**, ^{1}H and ^{13}C NMR spectra of compounds **3**, **5**, and **7**, UV/Vis and emission spectra of BBTTs **3**, **5**, and **7**, AIEE experiments, cyclic voltammetry of BBTTs **3**, **5**, and **7**, DFT computed XYZ-coordinates, energies, and absorption spectra of structures of selected BBTTs **3**, **5**, and **7**, NICS calculations of *anti-anti* BBTTs **7a**, **7c**, and **7e**, X-ray structure data tables.

Experimental Section

Synthesis of *N*-(4-*tert*-butylphenyl)bis[1]benzothieno[2,3-*b*:3',2'-*e*][1,4]thiazine (3a). A typical procedure. In a dry screw-cap Schlenk tube with a magnetic stir bar bis(3-bromobenzo[*b*]thiophene-2-yl)sulfane (**1**) (0.23 g, 0.50 mmol), bis(dibenzylideneacetone)palladium (22 mg, 0.038 mmol) and 1,1′-bis(dicyclohexylphosphano)ferrocene (43 mg, 0.074 mmol), and sodium *tert*-butoxide (0.14 g, 1.5 mmol) were placed under argon. 4-*tert*-Butyl-aniline (**2a**) (80 μL (0.50 mmol) and dry toluene (3 mL) were then added by syringe. The reaction mixture was stirred at 100 °C for 43 h. After cooling to room temperature a saturated aqueous sodium sulfite solution was added to the reaction mixture. The aqueous phase was extracted with dichloromethane (3 x 20 mL) and the combined organic phases were dried (anhydrous sodium sulfate). After evaporation of the solvents under reduced pressure the residue was absorbed on Celite®. The crude product was purified by flash chromatography on silica gel (cyclohexane) to give compound **3a** as a colorless solid (82 mg, 36%), Mp 175 °C. ^{1}H NMR (600 MHz, THF-d_8): δ 1.23 (s, 9 H), 6.80 – 6.83 (m, 2 H), 7.13 – 7.16 (m, 2 H), 7.35 – 7.38 (m, 2 H), 7.39 – 7.43 (m, 2 H), 7.82 – 7.85 (m, 4 H). ^{13}C NMR (151 MHz, THF-d_8): δ 31.9 (CH_3), 34.8 (C_{quat}), 117.1 (CH), 122.3 (CH), 123.9 (CH), 125.9 (CH), 125.9 (CH), 126.7 (CH), 132.4 (C_{quat}), 136.4 (C_{quat}), 139.8 (C_{quat}), 141.0 (C_{quat}), 144.6 (C_{quat}), 145.8 (C_{quat}). IR: $\tilde{\nu}$ [cm^{-1}] 3057 (w), 3034 (w), 2959 (w), 2899 (w), 2864 (w), 1611 (w), 1512 (m), 1472 (w), 1460 (w), 1427 (w), 1391 (w), 1350 (w), 1317 (w), 1286 (w), 1255 (w), 1246 (m), 1202 (w), 1173 (w), 1159 (w), 1130 (w), 1117 (w), 1090 (w), 1045 (w), 1018 (w), 1011 (w), 988 (m), 906 (w), 851 (w), 824 (m), 810 (w), 791 (w), 760 (s), 732 (s), 716 (w), 694 (w), 642 (w), 633 (w). HRMS (ESI) calcd. for $C_{26}H_{21}NS_3$: 443.0831; Found: 443.0831. Anal. calcd. for $C_{26}H_{21}NS_3$ (443.6): C 70.39, H 4.77, N 3.16, S 21.68. Found: C 70.20, H 4.88, N 3.11, S 21.45.

Synthesis of *N*-(4-*tert*-butylphenyl)bis[1]benzothieno[2,3-*b*:2',3'-*e*][1,4]thiazine (5a). A typical procedure. In a dry screw-cap Schlenk tube with a magnetic stir bar 2-bromo-3-((3-bromo-benzo[*b*]thiophen-2-yl)thio)benzo[*b*]thiophene (**4**) (0.23 g, 0.50 mmol)), bis(dibenzylideneacetone)palladium (22 mg, 0.038 mmol) and 1,1′-bis(dicyclohexylphosphano)ferrocene (43 mg, 0.074 mmol), and sodium *tert*-butoxide (0.14 g, 1.5 mmol) were placed under argon. 4-*tert*-Butyl-aniline (**2a**) (80 μL, 0.50 mmol) and dry toluene (3 mL) were then added by syringe. The reaction mixture was stirred at 110 °C for 47 h. After cooling to room temperature a saturated aqueous sodium sulfite solution was added to the reaction mixture. The aqueous phase was extracted with dichloromethane (3 x 20 mL) and the combined organic phases were dried (anhydrous sodium sulfate). After evaporation of the solvents under reduced pressure the residue was absorbed on Celite®. The crude product was purified by flash chromatography on silica gel (cyclohexane) to give compound **5a** after recrystallization from acetone as yellow crystals (104 mg, 47%), Mp 238 °C. ^{1}H NMR (600 MHz, THF-d_8): δ 1.32 (s, 9 H), 6.93 – 6.97 (m, 1 H), 7.07 – 7.12 (m, 1 H), 7.18 – 7.22 (m, 1 H), 7.24 – 7.29 (m, 1 H), 7.34 – 7.38 (m, 1 H), 7.39 – 7.42 (m, 1 H), 7.42 – 7.48 (m, 4 H), 7.67 – 7.71 (m, 1 H), 7.72 – 7.75 (m, 1 H). ^{13}C NMR (151 MHz, THF-d_8): δ 31.8 (CH_3), 35.3 (C_{quat}), 109.4 (C_{quat}), 120.5 (CH), 121.3 (C_{quat}), 122.0 (CH), 123.3 (CH), 123.5 (CH), 125.1 (CH), 125.2 (CH), 125.2 (CH), 125.4 (CH), 126.0 (CH), 127.4 (CH), 134.1 (C_{quat}), 135.6 (C_{quat}), 136.0 (C_{quat}), 136.5 (C_{quat}), 140.0 (C_{quat}), 144.5 (C_{quat}), 145.7 (C_{quat}), 150.0 (C_{quat}). IR: $\tilde{\nu}$ [cm^{-1}] 2965 (w), 2901 (w), 2868 (w), 1566 (s), 1557 (w), 1537 (w), 1508 (m), 1456 (w), 1431 (m), 1348 (m), 1256 (w), 1231 (w), 1204 (w), 1159 (m), 1115 (m), 1067 (m), 1051 (w), 1014 (w), 959 (w), 930 (w), 843 (m), 822 (w), 791 (w), 750 (s), 723 (s), 691 (w), 625 (w), 612 (w). MS (EI) (70 eV, *m/z* (%)): 443 ($[C_{26}H_{21}NS_3]^+$, 100), 428 ($[C_{25}H_{18}NS_3]^+$, 6), 386 ($[C_{22}H_{12}NS_3]^+$, 4), 310

($[C_{23}H_{21}NS_3]^+$, 86), 57 ($[C_4H_9]^+$, 57). Anal. calcd. for $C_{26}H_{21}NS_3$ (443.6): C 70.39, H 4.77, N 3.16, S 21.68. Found: C 70.55, H 4.68, N 3.14, S 21.74.

Synthesis of *N*-(4-*tert*-butylphenyl)bis[1]benzothieno[3,2-*b*:2',3'-*e*][1,4]thiazine (7a). A typical procedure. In a dry screw-cap Schlenk tube with a magnetic stir bar 2-bromo-3-((3-bromo-benzo[*b*]thiophen-2-yl)thio)benzo[*b*]thiophene (**6**) (0.23 g, 0.50 mmol)), bis(dibenzylideneacetone)palladium (22 mg, 0.038 mmol), 1,1′-bis(diphenylphosphano)ferrocene (42 mg, 0.076 mmol), and sodium *tert*-butoxide (0.14 g, 1.5 mmol) were placed under argon. 4-*tert*-Butyl-aniline (**2a**) (80 μL, 0.50 mmol) and dry toluene (3 mL) were then added by syringe. The reaction mixture was stirred at 100 °C for 44 h. After cooling to room temperature a saturated aqueous sodium sulfite solution was added to the reaction mixture. The aqueous phase was extracted with dichloromethane (3 x 20 mL) and the combined organic phases were dried (anhydrous sodium sulfate). After evaporation of the solvents under reduced pressure the residue was absorbed on Celite®. The crude product was purified by flash chromatography on silica gel (*n*-hexane/triethylamine 100:3) to give compound **7a** after recrystallization from acetone as orange crystals (127 mg, 57%), Mp 279 °C. ^{1}H NMR (600 MHz, THF-d_8): δ 1.40 (s, 9 H), 7.15 – 7.20 (m, 2 H), 7.29 – 7.32 (m, 2 H), 7.33 – 7.37 (m, 2 H), 7.56 – 7.60 (m, 4 H), 7.62 – 7.66 (m, 2 H). ^{13}C NMR (151 MHz, THF-d_8): δ 31.8 (CH_3), 35.8 (C_{quat}), 99.8 (C_{quat}), 120.1 (CH), 122.8 (CH), 124.0 (CH), 126.0 (CH), 128.3 (CH), 129.1 (CH), 134.6 (C_{quat}), 137.3 (C_{quat}), 141.2 (C_{quat}), 142.8 (C_{quat}), 153.9 (C_{quat}). IR: $\tilde{\nu}$ [cm^{-1}] 3065 (w), 2959 (w), 2901 (w), 2864 (w), 1595 (w), 1568 (m), 1508 (s), 1454 (m), 1437 (s), 1364 (w), 1288 (m), 1275 (s), 1244 (m), 1184 (m), 1159 (w), 1128 (w), 947 (w), 928 (w), 845 (m), 791 (w), 739 (s), 719 (s), 640 (w), 602 (m). MS (EI) (70 eV, *m/z* (%)): 443 ($[C_{26}H_{21}NS_3]^+$, 2), 310 ($[C_{16}H_8NS_3]^+$, 3), 298 (15), 297 (20), 296 ($[C_{26}H_8S_3]^+$, 100), 251 (8), 148 ($[C_9H_8S]^+$, 20). Anal. calcd. for $C_{26}H_{21}NS_3$ (443.6): C 70.39, H 4.77, N 3.16, S 21.68. Found: C 70.32, H 4.79, N 3.02, S 21.97.

Acknowledgments

The authors gratefully acknowledge the support by the Fonds der Chemischen Industrie, and Tobias Wilcke for the photographs, and the Hamamatsu Photonics Deutschland GmbH for measuring the absolute fluorescence quantum yields.

Keywords: Absorption • Aggregation induced emission enhancement • Antiaromaticity • Buchwald-Hartwig coupling • Cyclic voltammetry • DFT calculations • Fluorescence • Heterocycles • Polymorphism • 1,4-Thiazines

References:

[1] a) C.-T. Chen, *Chem. Mater.* **2004**, *16*, 4389 – 4400; b) Y. Ahn, D. E. Jang, Y.-B. Cha, M. Kim, K.-H. Ahn, Y. C. Kim, *Bull. Korean Chem. Soc.* **2013**, *34*, 107 – 111; c) J. K. Salunke, F. L. Wong, K. Feron, S. Manzhos, M. F. Lo, D. Shinde, A. Patil, C. S. Lee, V. A. L Roy, P. Sonar, P. P. Wadgaonkar, *J. Mater. Chem. C* **2016**, *4*, 1009 – 1018; d) Y. Park, B. Kim, C. Lee, A. Hyun, S. Jang, J.-H. Lee, Y.-S. Gal, T. H. Kim, K.-S. Kim, J. Park, *J. Phys. Chem. C* **2011**, *115*, 4843 – 4850; e) C. Poriel, J. Rault-Berthelot, S. Thiery, C. Quinton, O. Jeannin, U. Biapo, D. Tondelier, B. Geffroy, *Chem. Eur. J.* **2016**, *22*, 17930 – 17935; f) S. Feng, Q.-S. Li, T. A. Niehaus, Z.-S. Li, *Org. Electron.* **2017**, *42*, 234 – 243.

[2] a) R. Rybakiewicz, M. Zagorska, A. Pron, *Chem. Pap.* **2017**, ***71***, 243 – 268; b) K. Y. Chiu, T. T. H. Tran, C.-G. Wu, S.-H. Chang, T.-F. Yang, Y. O. Su, *J. Electroanal. Chem.* **2017**, *787*, 118 – 124; c) J. Wang, K. Liu, L. Ma, X. Zhan, *Chem. Rev.* **2016**, *116*, 14675 – 14725; d) E. Mondal, W.-Y. Hung, K.-T. Lin, H.-F. Chen, K.-T. Wong, *Org. Electron.* **2016**, *37*, 115 – 125; e) H. Bin, Y. Ji, Z. Li, N. Zhou, W. Jiang, Y. Feng, B. Lin, Y. Sun, *J. Lumin.* **2017**, *187*, 414 – 420; f) Y. Wang, Y. Zhu, G. Xie, H. Zhan, C. Yang, Y. Cheng, *J. Mater. Chem. C* **2017**, **5**, 10715 – 10720.

[3] I. S. Pereţeanu, T. J. J. Müller, *Org. Biomol. Chem.* **2013**, *11*, 5127 – 5135.

[4] B. Varga, Á. Csonka, A. Csonka, J. Molnár, L. Amaral, G. Spengler, *Anticancer Res.* **2017**, *37*, 5983 – 5993.

[5] a) R. Y. Lai, X. Kong, S. A. Jenekhe, A. J. Bard, *J. Am. Chem. Soc.* **2003**, 125, 12631 – 12639; b) T. Meyer, D. Ogermann, A. Pankrath, K. Kleinermanns, T. J. J. Müller, *J. Org. Chem.* **2012**, *77*, 3704 – 3715; c) Z.-S. Huang, H. Meier, and D. Cao, *J. Mater. Chem. C* **2016**, *4*, 2404 – 2426.

[6] a) C. Dostert, C. Wanstrath, W. Frank, T. J. J. Müller, *Chem. Commun.* **2012**, *48*, 7271 – 7273; b) C. Dostert, D. Czajkowski, T. J. J. Müller, *Synlett* **2014**, *25*, 371 – 374; c) C. Dostert, T. J. J. Müller, *Org. Chem. Front.* **2015**, *2*, 481 – 491; d) A. Schneeweis, A. Neidlinger, G. J. Reiss, W. Frank, K. Heinze, T. J. J. Müller, *Org. Chem. Front.* **2017**, *4*, 839 – 846.

[7] a) U. H. F. Bunz, J. U. Engelhart, B. D. Lindner, M. Schaffroth, *Angew. Chem. Int. Ed.* **2013**, *52*, 3810 – 3821; b) J. E. Anthony, *Chem. Rev.* **2006**, *106*, 5028 – 5048; c) U. H. F. Bunz, *Acc. Chem. Res.* **2015**, *48*, 1676 – 1686; d) Y. Li, Z. Wang, C. Zhang, P. Gu, W. Chen, H. Li, J. Lu, Q. Zhang, *ACS Appl. Mater. Interfaces* **2018**, 10, 15971 – 15979.

[8] a) X. Wang, F. Zhang, J. Liu, R. Tang, Y. Fu, D. Wu, Q. Xu, X. Zhuang, G. He, X. Feng, *Org. Lett.* **2013**, *15*, 5714 – 5717; b) H. Dong, C. Wang, W. Hu, *Chem. Commun.* **2010**, *46*, 5211 – 5222; c) C.-L. Chung, H.-C. Chen, Y.-S. Yang, W.-Y. Tung, J.-W. Chen, W.-C. Chen, C.-G. Wu, K.-T. Wong, *ACS Appl. Mater. Interfaces* **2018**, *10*, 6471 – 6483; d) C. Du, Y. Guo, Y. Liu, W. Qiu, H. Zhang, X. Gao, Y. Liu, T. Qi, K. Lu, G. Yu, *Chem. Mater.* **2008**, *20*, 4188 – 4190.

[9] a) J. P. Wolfe, R. A. Rennels, S. L. Buchwald, *Tetrahedron*, **1996**, *52*, 7525 – 7546; b) K. Nozaki, K. Takahashi, K. Nakano, T. Hiyama, H.-Z. Tang, M. Fujiki, S. Yamaguchi, K. Tamao, *Angew. Chem., Int. Ed.* **2003**, *42*, 2051 – 2053; c) M. Abboud, E. Aubert, V. Mamane, *Beilstein J. Org. Chem.* **2012**, *8*, 253 – 258; d) G. Koeckelberghs, L. De Cremer, W. Vanormelingen, W. Dehaen, T. Verbiest, A. Persoons, C. Samyn, *Tetrahedron* **2005**, *61*, 687 – 691.

[10] a) L. Jiang, S. L. Buchwald, *Palladium-Catalyzed Aromatic Carbon-Nitrogen Bond Formation*, Wiley-VCH Verlag GmbH, **2008**; b) J. F. Hartwig, *Synlett* **2006**, 1283 – 1294.

[11] a) Y. Ren, T. Baumgartner, *Chem. Asian J.* **2010**, *5*, 1918 – 1929; b) T. Yamamoto, S. Ogawa, R. Sato, *Tetrahedron Lett.* **2004**, *45*, 7943 – 7946; c) R. P. Dickinson, B. Iddon, *J. Chem. Soc. C* **1968**, 2733 – 2737.

[12] Crystallographic data (excluding structure factors) for the structures reported in this paper have been deposited with the Cambridge Crystallographic Data Centre as supplementary publication nos. CCDC-1851241 (**3a**), 1851244 (**3d**), 1851247 & 1851248 (**5d**), 1851249 (**7a**),

1851250 (**7c**), 1851251 (**7d**) and 1851252 (**7e**). Copies of the data can be obtained free of charge on application to CCDC, 12 Union Road, Cambridge CB2 1EZ, UK (Fax: + 44-1223/336-033; E-mail: deposit@ccdc.cam.ac.uk).

[13] P. De Meester, S. S. C. Chu, M. V. Jovanovic, E. R. Biehl, *Acta Cryst. C* **1986**, *42*, 1794 – 1797.

[14] C. L. Klein, J. M. Conrad III, S. A. Morris, *Acta Cryst. C* **1985**, *41*, 1202 – 1204.

[15] a) G. Fronza, R. Mondelli, G. Scapini, G. Ronsisvalle, F. Vittorio, *J. Magn. Reson.* **1976**, *23*, 437 – 454; b) P. Borowicz, J. Herbich, A. Kapturkiewicz, R. Anulewicz Ostrowska, J. Nowacki, G. Grampp, *Phys. Chem. Chem. Phys.* **2000**, *2*, 4275 – 4280; c) M. V. Jovanovic, E. R. Biehl, P. De Meester, S. S. C. Chu, *J. Heterocycl. Chem.* **1984**, *21*, 1793 – 1800; d) C. Besnard, C. Kloc, T. Siegrist, K. Pluta, *J. Chem. Crystallogr*. **2005**, *35*, 731 – 736; e) M. V. Jovanovic, E. R. Biehl, P. De Meester, S. S. C. Chu, *J. Heterocycl. Chem.* **1984**, *21*, 885 – 888.

[16] a) A. Bondi, *J. Phys. Chem.* **1964**, **68**, 441 – 451. b) S.-Z. Hu, Z.-H. Zhou, Z.-X. Xie, E. Robertson Beverly, *Z. Kristallog. – Cryst. Mater*. **2014**, *229*, 517 – 523.

[17] a) C. F. Marcos, T. Torroba, O. Rakitin, C. W. Rees, A. J. P. White, D. J. Williams, *Chem. Commun.* **1999**, 29 – 30; b) M. Nowak, K. Pluta, K. Suwińska, L. Straver, *J. Heterocycl. Chem.* **2007**, *44*, 543 – 550; c) K. Pluta, M. Nowak, K. Suwińska, *J. Chem. Crystallogr*. **2000**, *30*, 479 – 482.

[18] a) P. v. R. Schleyer, C. Maerker, A. Dransfeld, H. Jiao, N. J. R. van Eikema Hommes, *J. Am. Chem. Soc*. **1996**, *118*, 6317 – 6318; b) Z. Chen, C. S. Wannere, C. Corminboeuf, R. Puchta, P. v. R. Schleyer, *Chem. Rev.* **2005**, *105*, 3842 – 3888; c) U. Fleischer, W. Kutzelnigg, P. Lazzeretti, V. Muehlenkamp, *J. Am. Chem. Soc*. **1994**, *116*, 5298 – 5306; d) P. v. R. Schleyer, H. Jiao, N. J. R. v. E. Hommes, V. G. Malkin, O. L. Malkina, *J. Am. Chem. Soc*. **1997**, *119*, 12669 – 12670; e) P. v. R. Schleyer, M. Manoharan, Z.-X. Wang, B. Kiran, H. Jiao, R. Puchta, N. J. R. van Eikema Hommes, *Org. Lett*. **2001**, *3*, 2465 – 2468; f) H. Fallah-Bagher-Shaidaei, C. S. Wannere, C. Corminboeuf, R. Puchta, P. v. R. Schleyer, *Org. Lett.* **2006**, *8*, 863 – 866; g) T. Nishinaga, T. Ohmae, M. Iyoda, *Symmetry* **2010**, *2*, 76 – 97; h) A. Stanger, *J. Org. Chem.* **2006**, *71*, 883 – 893; i) J. Cao, G. London, O. Dumele, M. von Wantoch Rekowski, N. Trapp, L. Ruhlmann, C. Boudon, A. Stanger, F. Diederich, *J. Am. Chem. Soc.* **2015**, *137*, 7178 – 7188; j) N. S. Mills, M. Benish, *J. Org. Chem.* **2006**, *71*, 2207 – 2213; k) Chaolumen, M. Murata, A. Wakamiya, Y. Murata, *Org. Lett.* **2017**, *19*, 826 – 829; l) G. V. Baryshnikov, R. R. Valiev, N. N. Karaush, B. F. Minaev, *Phys. Chem. Chem. Phys.* **2014**, *16*, 15367 – 15374; m) X. Wang, Z. Zhang, Y. Song, Y. Su, X. Wang, *Chem. Commun.* **2015**, *51*, 11822 – 11825; n) J. Liu, J. Ma, K. Zhang, P. Ravat, P. Machata, S. Avdoshenko, F. Hennersdorf, H. Komber, W. Pisula, J. J. Weigand, A. A. Popov, R. Berger, K. Müllen, X. Feng, *J. Am. Chem. Soc.* **2017**, *139*, 7513 – 7521.

[19] M. J. Frisch, G. W. Trucks, H. B. Schlegel, G. E. Scuseria, M. A. Robb, J. R. Cheeseman, G. Scalmani, V. Barone, B. Mennucci, G. A. Petersson, H. Nakatsuji, M. Caricato, X. Li, H. P. Hratchian, A. F. Izmaylov, J. Bloino, G. Zheng, J. L. Sonnenberg, M. Hada, M. Ehara, K. Toyota, R. Fukuda, J. Hasegawa, M. Ishida, T. Nakajima, Y. Honda, O. Kitao, H. Nakai, T. Vreven, J. A. Montgomery, Jr., J. E. Peralta, F. Ogliaro, M. Bearpark, J. J. Heyd, E. Brothers, K. N. Kudin, V. N. Staroverov, R. Kobayashi, J. Normand, K. Raghavachari, A. Rendell, J. C. Burant, S. S. Iyengar, J. Tomasi, M. Cossi, N. Rega, J. M. Millam, M. Klene, J. E. Knox, J. B. Cross, V. Bakken, C. Adamo, J. Jaramillo, R. Gomperts, R. E. Stratmann, O. Yazyev, A. J. Austin, R. Cammi, C. Pomelli, J. W. Ochterski, R. L. Martin, K. Morokuma, V. G. Zakrzewski, G. A. Voth, P. Salvador, J. J. Dannenberg, S. Dapprich, A. D. Daniels, O. Farkas, J. B. Foresman, J. V. Ortiz, J. Cioslowski, D. J. Fox, *GAUSSIAN 09* (*Revision A.02*) Gaussian, Inc., Wallingford CT, **2009**.

[20] a) A. D. Becke, *J. Chem. Phys.* **1993**, *98*, 5648 – 5652; b) A. D. Becke, *J. Chem. Phys.* **1993**, *98*, 1372 – 1377.

[21] a) R. Krishnan, J. S. Binkley, R. Seeger, J. A. Pople, *J. Chem. Phys.* **1980**, *72*, 650 – 654; b) A. D. McLean, G. S. Chandler, *J. Chem. Phys.* **1980**, *72*, 5639 – 5648.

[22] R. Wolfe, E. Culver, S. Rasmussen, *Molecules* **2018**, *23*, 2279.

[23] I. Noviandri, K. N. Brown, D. S. Fleming, P. T. Gulyas, P. A. Lay, A. F. Masters, L. Phillips, *J. Phys. Chem. B* **1999**, *103*, 6713 – 6722.

[24] G. Gritzner, J. Kůta, *Electrochim. Acta* **1984**, *29*, 869 – 873.

[25] L. Michaelis, *Chem. Rev*. **1935**, *16*, 243 – 286.

[26] a) M. I. Pilo, G. Sanna, R. Seeber, *J. Electroanal. Chem.* **1992**, *323*, 103 – 115; b) J.-S. Yu, Z.-X. Zhang, *J. Electroanal. Chem.* **1996**, *403*, 1 – 9; c) C. L. Bentley, A. M. Bond, A. F. Hollenkamp, P. J. Mahon, J. Zhang, *Anal. Chem.* **2014**, *86*, 2073 – 2081; d) A. Obaid, E. El-Mossalamy, S. Al-Thabaiti, I. El-Hallag, A. Hermas, A. Asiri, *Int. J. Electrochem. Sci.* **2014**, *9*, 1003 – 1015; e) H. L. Surprenant, T. H. Ridgway, C. N. Reilley, *J. Electroanal. Chem. Interfacial Electrochem.* **1977**, *75*, 125 – 134; f) E. H. El-Mossalamy, A. Y. Obaid, S. A. El-Daly, I. S. El-Hallag, A. M. Asiri, L. M. Al-Harbi, *J. New Mater. Electrochem. Syst.* **2013**, *16*, 53 – 57; g) R. Abdel-Hamid, M. K. M. Rabia, A.-B. M. El-Nady, *Talanta* **1994**, *41*, 1453 – 1458; h) I. S. El-Hallag, *J. Chil. Chem. Soc.* **2010**, *55*, 67 – 73.

[27] U. Tokiko, I. Masanori and K. Kozo, *Bull. Chem. Soc. Jpn.* **1983**, *56*, 577 – 582.

[28] a) M. Hauck, M. Stolte, J. Schönhaber, H. G. Kuball, T. J. J. Müller, *Chem. Eur. J.* **2011**, *17*, 9984 – 9998; b) L. Yang, J.-K. Feng, A.-M. Ren, *J. Org. Chem.* **2005**, *70*, 5987 – 5996.

[29] A. Bejan, S. Shova, M.-D. Damaceanu, B. C. Simionescu, L. Marin, *Crystal Growth & Design* **2016**, *16*, 3716 – 3730.

[30] N. Boens, W. Qin, N. Basarić, J. Hofkens, M. Ameloot, J. Pouget, J.-P. Lefèvre, B. Valeur, E. Gratton, M. vandeVen, N. D. Silva, Y. Engelborghs, K. Willaert, A. Sillen, G. Rumbles, D. Phillips, A. J. W. G. Visser, A. van Hoek, J. R. Lakowicz, H. Malak, I. Gryczynski, A. G. Szabo, D. T. Krajcarski, N. Tamai, A. Miura, *Anal. Chem.* **2007**, *79*, 2137 – 2149.

[31] a) H. Langhals, T. Potrawa, H. Nöth, G. Linti, *Angew. Chem. Int. Ed.* **1989**, *28*, 478 – 480; b) T. Mutai, H. Satou, K. Araki, *Nat. Mater*. **2005**, *4*, 685 – 687; c) G. Zhang, J. Lu, M. Sabat, C. L. Fraser, *J. Am. Chem. Soc.* **2010**, *132*, 2160–2162.

[32] a) V. D. Singh, R. S. Singh, R. P. Paitandi, B. K. Dwivedi, B. Maiti, D. S. Pandey, *J. Phys. Chem. C* **2018**, *122*, 5178 – 5187; b) J. Mei, N. L. C. Leung, R. T. K. Kwok, J. W. Y. Lam, B. Z. Tang, *Chem. Rev.* **2015**, *115*, 11718 – 11940; c) Y. Hong, J. W. Y. Lam, B. Z. Tang, *Chem. Soc. Rev.* **2011**, *40*, 5361 – 5388; d) Y. Hong, J. W. Y. Lam, B. Z. Tang, *Chem. Commun.* **2009**, 4332 – 4353; e) B. Z. Tang, X. Zhan, G. Yu, P. P. Sze Lee, Y. Liu, D. Zhu, *J. Mater. Chem.* **2001**, *11*, 2974 – 2978; f) J. Luo, Z. Xie, J. W. Y. Lam, L. Cheng, H. Chen, C. Qiu, H. S. Kwok, X. Zhan, Y. Liu, D. Zhu, B. Z. Tang, *Chem. Commun.* **2001**, 1740 – 1741; g) J. Yang, J. Huang, Q. Li, Z. Li, *J. Mater. Chem. C* **2016**, *4*, 2663 – 2684.

[33] a) Q. Qi, Y. Liu, X. Fang, Y. Zhang, P. Chen, Y. Wang, B. Yang, B. Xu, W. Tian and S. X.-A. Zhang, *RSC Advances* **2013**, *3*, 7996 – 8002. b) Q. Zeng, Z. Li, Y. Dong, C. A. Di, A. Qin, Y. Hong, L. Ji, Z. Zhu, C. K. W. Jim, G. Yu, Q. Li, Z. Li, Y. Liu, J. Qin and B. Z. Tang, *Chem. Commun.* **2007**, 70 – 72.

[34] S. M. Borisov, O. S. Wolfbeis, *Chem. Rev.* **2008**, *108*, 423 – 461.

10.1002/chem.201805085

WILEY-VCH

Entry for the Table of Contents

FULL PAPER

Bis[1]benzothieno[1,4]thiazines (BBTT) are a novel class of anellated thiazines with remarkable features: *anti-anti* BBTTs are planar according to X-ray structure analysis and NICS calculations support an antiaromatic character; all BBTT show high radical cation stabilities and lower oxidation potentials than phenothiazines; depending on the anellation mode solid state luminescence and even aggregation induced emission enhancement is found.

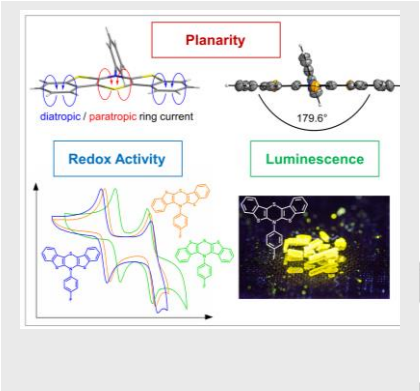

Arno P. W. Schneeweis,[a] Simone T. Hauer,[a] Guido J. Reiss,[b] and Thomas J. J. Müller[a]*

Page No. – Page No.

Bis[1]benzothieno[1,4]thiazines – Planarity, Enhanced Redox Activity and Luminescence by Thieno-Expansion of Phenothiazine